

Unlocking Versatile Locomotion: A Novel Quadrupedal Robot with 4-DoFs Legs for Roller Skating

Jiawei Chen¹, Ripeng Qin², Longfei Huang^{1,3}, Zongbo He^{1,3},

Kun Xu^{1*}, *Member IEEE*, and Xilun Ding¹

Abstract—Roller skating with passive wheels on a quadrupedal robot is more efficient than traditional walking. However, the typical mammalian quadruped robot with 3-DoFs legs can only perform one dynamic roller skating gait and has difficulty achieving turning motion. To address this limitation, we designed a novel quadrupedal robot with each leg having 4-DoFs to enable various roller skating locomotion including Swizzling, Stroking, and trot-like gaits while easily achieving turning motions. We considered the geometrical characteristics of the passive wheel and used the Levenberg-Marquardt method in robot kinematics to improve precision for both roller skating kinematics and contact point position for the dynamics controller. The position of the robot foot and the yaw angle of the passive wheel are decoupled for motion planning of all proposed gaits. Our proposed kinematics with wheeled geometry was verified through experiments to have higher precision, while the feasibility of all proposed roller-skating gaits was confirmed during straight motion and turning motion with a small radius on our prototype robot. Finally, we discussed the mobility efficiency of different roller skating gaits which were found to be more efficient than walking.

I. INTRODUCTION

Passive wheels enable humans to achieve complex and dynamic roller skating at high speeds on the ground, providing an ideal model for robots seeking to improve their mobile efficiency through passive wheel roller skating.

While humans with seven degrees of freedom (DoFs) in their legs can execute intricate roller skating maneuvers, typical mammalian robots with only three DoFs per leg struggle to perform complex gaits and turning motions. To address this limitation, we added an active DoF to each leg of our quadrupedal robot QSkater[1], resulting in a new design called QSkater-E that incorporates passive wheels. With the addition of a fourth degree of freedom, this robot is capable of executing multiple roller skating gaits while easily achieving turning motions.

A. Related Works

The wheel-legged quadrupedal robot that has both the high adaptability of legged robots and the high mobility of

wheeled robots has always been a hot topic in the field of robot research. According to the fitting method between leg and wheel, the wheel-legged quadrupedal robot[2] can be divided into Leg-wheel fusion type and Independent leg-wheel type. With the improvement of quadruped robot technology, the leg-wheel fusion type quadrupedal robot become the mainstream, such as the famous robot Anymal. Anymal[3-5] with wheels, has achieved a trajectory optimizer using linearized ZMP constraints to a compound motion of actuated wheels and legs. A wheel motion generator[6, 7] is proposed to track the centroidal motion of one quadruped-on-wheel robot which can cross various rough terrains with the model-based whole-body torque control. Complios[8] can spontaneously adapt its configuration while it is rolling on unknown uneven terrain and give access to the measurement of horizontal forces applied on the legs, which constitutes valuable information when it comes to choosing an appropriate response during obstacle crossing. CENTAURO[9, 10] is a centaur-like body that is controlled by a torque-compliant actuator and four articulated legs ending in steerable wheels allow for omnidirectional driving as well as for making steps. A dual-frequency gait planning method[11] which controls the robot's gait cycle's duty factor and generates unique turning gait patterns for wheel locomotion is proposed. A control framework[12] to tackle the hybrid locomotion problem of wheeled-legged robots is proposed and is demonstrated by the simulation.

Based on the driving form of the wheel, the wheel-legged quadrupedal robot can be divided into quadrupedal robots with active and passive wheels. Although the active wheel which holds its position can be similar to the foot, the contact force can easily make the actual wheel rotate and the wheel affects the dynamic characteristics of the legs while the robot is walking. The method to control the quadrupedal robot with passive wheels for roller skating is an interesting topic because of the non-holonomic constraints produced by passive wheels. The roller skating static gait similar to the human Swizzling gait using kinematic control has been achieved for the Roller-Walker[13] with passive wheels. The special quadrupedal robot, Anymal with passive wheels, can achieve a static roller skating gait[14] which can skate on flat and inclined terrain with force control. Skaterbots[15] and AgileBot[16] whose leg has 4 DoFs can achieve a Swizzling gait similar to Roller-Walker and a Stroking gait similar to the trot. Skaterbots used a computation-driven approach to locomote with arbitrary arrangements of legs and wheels.

The work is supported by the National Natural Science Foundation of China (Grant No. 52375003, and Grant No. T2121003).

*Corresponding author: Kun Xu (e-mail: xk007@buaa.edu.cn)

¹School of Mechanical Engineering and Automation, Beihang University, 37 Xueyuan Road, Beijing, 100191, China

²School of Mechanical Engineering at Inner Mongolia University of Science and Technology, China

³Beijing Institute of Spacecraft System Engineering, China

Similar to the walking gaits, the skating gaits of a quadrupedal robot can be divided into static skating gait and dynamic skating gait. The static/dynamic skating gait is defined as the robot/human being in a statically/dynamically stable state while skating. A dynamic roller-skating gait[17] of the quadrupedal robot with passive wheels which is imitated by human roller skating proposed to promote mobile efficiency.

B. Contribution

In this paper, we dedicate ourselves to the versatile roller skating gaits on one quadrupedal robot. The main contributions of this paper are:

1) A novel quadrupedal robot whose each leg has 4-DoFs with passive wheels is designed and can achieve walking and multiple roller skating gaits (Swizzling, Stroking, and trot-like).

2) A passive wheel model with geometrical characteristics is proposed to improve precision in both roller skating kinematics and contact point position for dynamics controller using the Levenberg-Marquardt method in the robot kinematics.

3) Finally, the proposed locomotion design is verified on the robot prototype “QSkater-E” through experiments. The experiment result shows the locomotion design has high precision and the robot can achieve multiple roller skating gaits with a small radius. The COT of the multiple roller skating gaits is significantly lower than that of the walking.

II. ROBOT STRUCTURE AND MODEL

A. The whole structure of the robot

The quadrupedal robot with the passive wheel-foot effector named “QSkater-E” consists of one body and four legs and its mechanism sketch is demonstrated in Fig. 1. Each leg has four active DoFs and one passive DoF (one passive wheel). The fixed ground coordinate system is denoted by the ground coordinate system (S) and is used for the route design. The moving coordinate system located at the geometric center of the body is denoted by the body coordinate system (M).

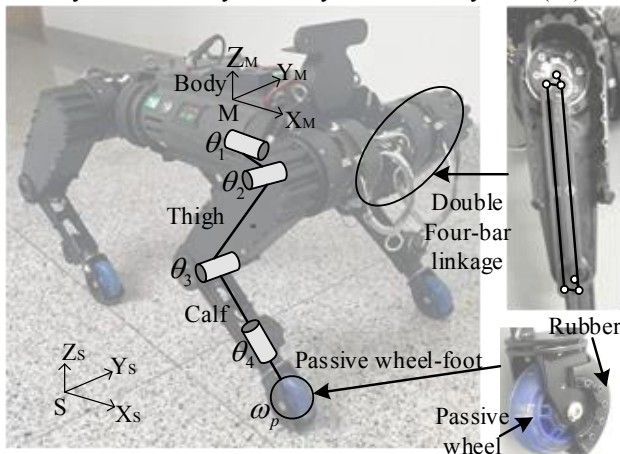


Fig. 1 Sketch of the quadrupedal robot with passive wheel-foot effector named “QSkater-E”. $\theta_1, \theta_2, \theta_3, \theta_4$ and ω_p are the angles of active joints and the angular speed of passive wheel on each leg of the robot.

To reduce the moments of the leg, the four-bar linkage is

designed to deploy the motor to the root of the leg. The double parallel four-bar linkage[18] is used to avoid the singular configuration. The ingenious passive wheel-foot effector uses a passive wheel as the inner core which is wrapped by a rubber cover. The passive wheel-foot effector can be regarded as the flexible foot when the rubber contacts the ground, otherwise, it can be regarded as a passive wheel.

There are two modes of the proposed robot: the walking mode and the skating mode shown in Fig. 2. According to the contact characteristic between the wheel-foot effector and the ground, the leg can be divided into walking and skating mode. The robot can choose the contact between the passive wheel-foot effector and the ground to achieve roller skating and walking. While the robot is walking, the contact part between the wheel-foot effector and the ground is the rubber which is the same as the one of the quadrupedal robot. While the robot is skating, the contact part between the wheel-foot effector and the ground is the passive wheel.

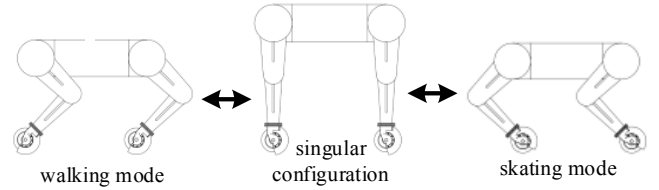


Fig. 2 Modes of the quadrupedal robot with passive wheel-foot. Two modes are the walking mode and the skating mode. Switching between modes can be achieved by passing through the singularity.

B. Kinematics of robot for roller skating

In our previous works, we used the type mammalian quadrupedal with passive wheels to achieve a unitary roller skating gait, and the passive wheels are regarded as a simple non-steerable model. Different from our previous works, the proposed quadrupedal robot utilizing the fourth joint of each leg can control the direction angle of the passive wheel to realize diverse roller skating locomotion.

Each leg of the proposed robot has one more active and passive DoF than the typical mammalian quadruped robot. In the waking mode, the proposed robot has the same configuration as the mammalian quadruped robot when the fourth active joint of each leg is fixed as zero. So, the kinematics of the robot in the walking is not discussed in detail.

In the skating mode, the passive wheel can not be directly controlled and the fourth active joint of each leg can be used to control the direction of the passive wheel. The contact model between the passive wheel-foot effector and the ground is used to build the kinematics of the robot shown in Fig. 3. The passive wheel is regarded as a non-steerable model with thickness. The moving coordinate system located at the geometric center of the passive wheel is denoted by the foot coordinate system (W). The axis of the passive wheel is the Y-axis of the foot coordinate system.

Forward Kinematics:

Using the product of exponential, the position and orientation of the W coordinate system can be obtained as

$$\mathbf{G}_W = \mathbf{G}_M e^{\theta_1 \xi_1} e^{\theta_2 \xi_2} e^{\theta_3 \xi_3} e^{\theta_4 \xi_4} \mathbf{G}_{W0} \quad (1)$$

where \mathbf{G}_M is the position and orientation of the robot body,

$\xi_1, \xi_2, \xi_3, \xi_4$ are the initial screw of active joints, and G_{W0} is the initial position and orientation of the W coordinate system relative to the body coordinate system.

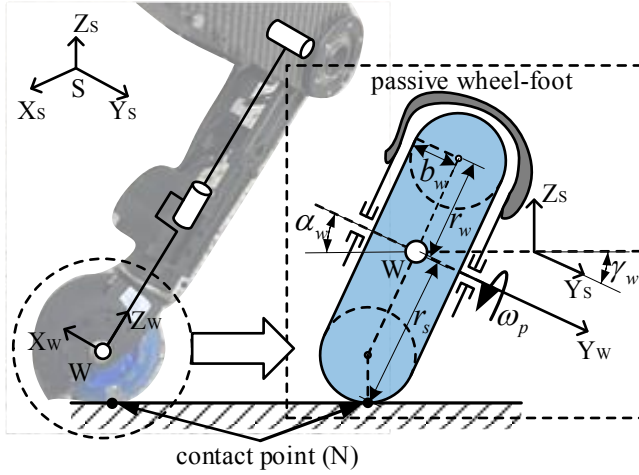


Fig. 3 The contact model between the passive wheel-foot effector and the ground. The geometric center of the passive wheel is the point W. The contact between the passive wheel and the ground is regarded as a point N. $b_w, r_w,$ and r_s are the half of width, equivalent radius and actual radius of the passive wheel, respectively. The orientation of the wheel can be described as: rotates γ_w around the Z-axis after rotating α_w around X-axis in the ground coordinate system. γ_w and α_w are defined as the yaw angle (direction angle) and roll angle of the passive wheel, respectively.

According to the definition of the wheel, the direction angle and the roll angle of the passive wheel can be expressed as:

$$\begin{cases} \gamma_w = -\arctan(g_{12}^W/g_{22}^W) & -90^\circ < \gamma_w < 90^\circ \\ \alpha_w = \arcsin(g_{32}^W) & -90^\circ < \alpha_w < 90^\circ \end{cases} \quad (2)$$

where g_{ab}^W is the elements of row a and column b of the G_W .

In most research, the wheel is regarded as a point W and the wheel geometry is not considered. However, the skating velocity is affected by the wheel geometry. In this paper, we consider the wheel geometry to improve the precision of roller skating kinematics and the contact point for the dynamics controller. Based on the wheel geometry, the position of the contact point N can be expressed as:

$$P_N = \begin{bmatrix} -r_w \sin \gamma_w \sin \alpha_w \\ r_w \cos \gamma_w \sin \alpha_w \\ -r_w \cos \alpha_w - b_w \end{bmatrix} + P_W \quad (3)$$

where P_W is the position of the W coordinate system.

Inverse Kinematics:

The direction angle and the contact point of the passive wheel are important for the roller-skating gait. For the inverse kinematics, the position of the contact point and the direction angle of the passive wheel are inputs to get the expected four joints of each leg. Because of the coupling and nonlinear relationship between four active joints, the direction angle, and the contact position of the passive wheel, the analytical solution is hard to get.

We use the numerical method for the inverse kinematics of each leg to obtain the precise solution. The nonlinear equations of the inverse kinematics can be expressed as:

$$\begin{cases} g_{12}^W \cos \gamma_w + g_{22}^W \sin \gamma_w = 0 \\ r_w \begin{bmatrix} g_{12}^W g_{32}^W \\ g_{22}^W g_{32}^W \\ g_{32}^W g_{32}^W - 1 \end{bmatrix} + \left(P_W - P_N - \begin{bmatrix} 0 \\ 0 \\ b_w \end{bmatrix} \right) \sqrt{1 - g_{32}^W g_{32}^W} = 0 \end{cases} \quad (4)$$

The Levenberg-Marquardt method is used to solve the inverse kinematics of each leg. The inverse kinematics with four equations and parameters has multiple solutions shown in Fig. 4. To avoid the singular solution and reduce iterations of the Levenberg-Marquardt method, the approximate solution that ignores the wheel geometry is utilized as the initial value. The approximate analytical solution of each leg can be divided into two steps: 1) The first three joints of each leg can be obtained by the inverse position solution of one mammalian leg when the contact point N is regarded as the point W. 2) The fourth joint can be obtained as:

$$\theta_4 = \arctan\left(\frac{r_{12} + r_{22} \tan \gamma_w}{r_{11} + r_{21} \tan \gamma_w}\right) - 90^\circ < \theta_4 < 90^\circ \quad (5)$$

where r_{ab} is the elements of row a and column b of the orientation matrix which can be got by the forward kinematics of the body orientation and the first three joints of each leg.

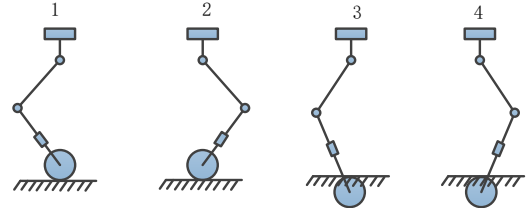


Fig. 4 The multiple solutions of the inverse kinematics of each leg.

C. Dynamics of robot for roller skating

The dynamics model of the quadrupedal robot based on the center of inertia (CoI) is selected as the dynamics model for the controller. There are only two external forces on the robot without consideration of external disturbance: the ground reaction force (GRF) and gravity. In the body frame, the dynamics model can be expressed as

$$M_c \dot{V}_M + \dot{M}_c V_M - \text{ad}_{V_M}^T M_c V_M = F_g + F_f \quad (6)$$

where M_c and \dot{M}_c are the inertia matrix and its differential of the whole robot relative to the body frame, V_M and \dot{V}_M are the twist and its differential of the body frame, F_g and F_f represent the wrench of the gravity and the GRF relative to the body frame. ad_{V_M} is the adjoint operator of the twist V_M . The body orientation and position are expressed as in the exponential mapping on $SE(3)$ for the trajectory design.

III. LOCOMOTION DESIGN

Utilizing the 4-DoFs leg, the robot can realize diverse roller skating locomotion including the Swizzling static gait, Stroking static gait, and trot-like dynamic gait.

The locomotion design of this robot for roller skating can be divided into two into two parts: the body trajectory and the passive wheel-foot trajectory. Different from our previous works, the trajectory design of the passive wheel contains the

contact position between the wheel and the ground and the direction angle of the wheel.

A. Direction angle of wheel-foot

When all direction angles of the supporting wheel-foot satisfy the nonholonomic constraint, the robot body can achieve stable skating motion. The constraint between the body and the direction angle of the supporting wheel shown in Fig. 5 can be expressed as

$$\mathbf{v}_p = \mathbf{v}_{NM} + \mathbf{v}_{fM} \quad (7)$$

$$\mathbf{v}_{fM} = [0 \ 0 \ \omega_{Mz}]^T \times \mathbf{p}_{NM} + [v_{Mx} \ 0 \ 0]^T \quad (8)$$

where $\mathbf{v}_{NM} = d\mathbf{p}_{NM}/dt$ can be obtained by the locomotion design of the contact position. The direction angle of the wheel-foot can be computed as the angle between the vector \mathbf{v}_p and the X-axis in the horizontal plane relative to the body coordinate system. For continuity, the direction angle of the swing wheel is calculated in the same way as the one of the supporting wheels.

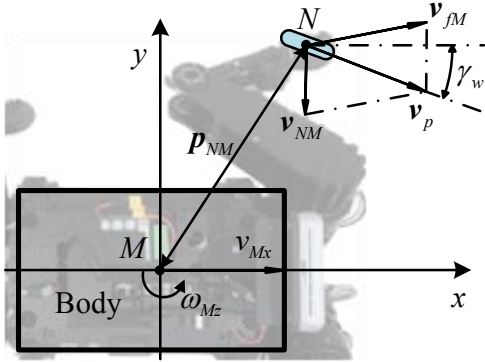


Fig. 5 The constraint between the body and the direction angle of the supporting wheel-foot. The expected linear velocity along the X-axis and the expected angular velocity along Z-axis relative to the body coordinate system is denoted as v_{Mx} and ω_{Mz} , respectively. \mathbf{p}_{NM} and \mathbf{v}_{NM} are the position and linear velocity of the contact point N relative to the body coordinate system. The linear velocity \mathbf{v}_{fM} is generated by the v_{Mx} and ω_{Mz} at the point N. \mathbf{v}_p is the linear velocity of the point N relative to the ground coordinate system.

B. Swizzling static gait of roller skating

The Swizzling static gait is inspired by the human Swizzling roller skating gait. In the Swizzling gait, all legs of the robot remain supporting and there is no swing leg. We divided the front and hind legs of the quadruped robot into two groups which is similar to human legs.

The locomotion of the front/hind legs shown in Fig. 6 can be divided into two phases: the push-out phase and the push-inward phase. The passive wheels of the front/hind legs in the transform state between the push-out and push-inward phase is a singular configuration. To avoid this singular configuration, the motion of the front and hind legs has a phase difference. We hope the cycle time of the gait is negatively correlated with the speed of the roller skating. So, the desired trajectory of the contact point can be expressed as

$$\mathbf{p}_{NM} = \mathbf{p}_{NM0} + \left[0 \ L_p \sin\left(\frac{2\pi}{T} \int_0^t v_{Mx} dt\right) \ 0 \right]^T \quad (9)$$

where \mathbf{p}_{NM0} is the initial desired contact position, L_p is the

lateral motion length, and T is the cycle time of the gait.

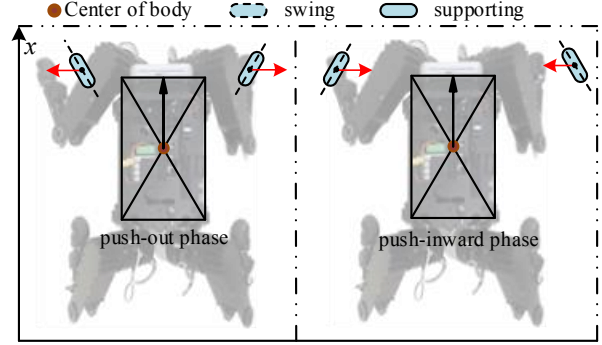


Fig. 6 The two phases of the Swizzling static gait. In the push-out phase, the wheel-foot of the front/hind legs moves outwards along the Y-axis of the body coordinate system. The push-inward phase is the opposite of the push-out phase.

C. Stroking static gait of roller skating

The stroking static gait imitates the human skateboarding motion which has a skating platform and uses one leg to generate thrust. In the stroking gait, the robot uses three legs to form a skating platform and one leg to generate thrust.

The stroking gait shown in Fig. 7 can be divided into two phases: the pushing phase and the skating phase.

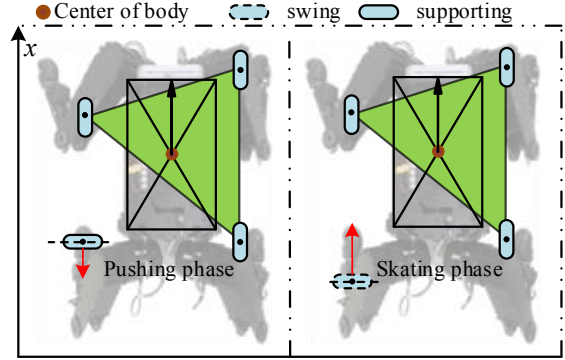


Fig. 7 The two phases of the Stroking static gait. In the pushing phase, one leg is used to push the ground to generate the power. In the skating phase, the robot with three supporting legs skates on the ground. In those phases, the center of mass of the robot body remains within the support polygon.

The direction angle of the passive wheel of the leg used to generate thrust is set at 90° . The position of the robot body and the three legs which are used to form the supporting polygon remain unchanged. The direction angle of the supporting legs is used to decide the skating motion and can be computed by Section III-A.

D. The trot-like gait of roller skating

The trot-like gait of the quadrupedal robot is a dynamic roller skating gait. Different from our previous works[19], the proposed robot whose direction angle of the passive wheels can be controlled is more flexible. The robot can use the direction angle of the wheels to achieve turning motion easily.

In the trot-like roller skating gait, the diagonal legs (left front and right hind, right front and left hind) have a similar motion and are named as one group leg. The one group of legs of the trot-like gait shown in Fig. 8 can be divided into two

phases.

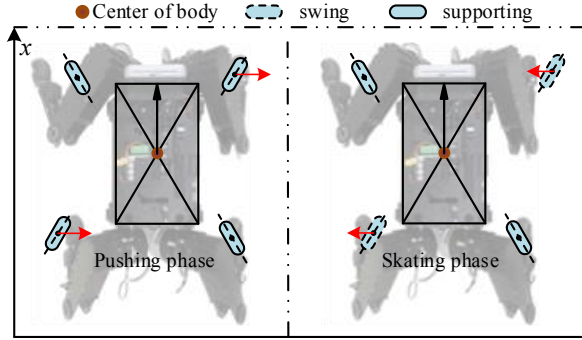


Fig. 8 The two phases of one group leg for the trot-like dynamic gait. In the pushing phase, the group of legs is used to push the ground to generate the power. In the skating phase, the group of legs swing back to the initial position and the robot skates with two supporting legs on the ground.

E. Motion Control

The motion control of the proposed robot can be divided into two parts:

1) The first three joints of each leg are used to control the orientation and position of the body and the foot position. First, the expected ground reaction force of supporting legs is obtained using the dynamics controller[1] based on the center of inertia on $SE(3)$. Then, the whole body control (WBC)[20] is selected to compute the expected angle, angular velocity, and torque. Last, the Field Oriented Control (FOC) is used to achieve the joint control.

2) The fourth joint of each leg is used to control the wheel direction angle. First, the expected angle of the fourth joint is obtained by the kinematics of Section III. Then, the Proportion-Differentiation (PD) controller is utilized to achieve the joint control.

IV. EXPERIMENTS

The experiments for the robot consist of three parts: the kinematics contrast experiment with the wheel geometry, the feasibility experiment of the roller skating gaits, and the energy consumption experiment between different roller skating gaits (All experiments video of the quadrupedal robot using the proposed controller is shown in the video). The important parameters of the quadrupedal robot with passive wheels are expressed in Table 1.

TABLE 1
QUADRUPEDAL ROBOT PARAMETERS

Robot parameter	Value
Body width	0.3 m
Body length	0.4 m
Thigh length	0.2 m
Calf length	0.2 m
passive wheels	$r_w = 0.027m, b_w = 0.005m$

The orientation and position of the robot body use the inertial measurement unit and the observability-constrained Extended Kalman Filter[21]. The Robot Operating System (ROS) is used as the control system and the qpOASES is used for solving the optimization.

A. Kinematics contrast experiment

The kinematics contrast experiment compares whether to

consider the wheel geometry of each leg for the skating motion on the robot prototype. The position of the contact point and yaw of the wheel on the robot prototype using the trajectory of the Swizzling gait is shown in Fig. 9. In Fig. 9, the contact point trajectory and the yaw of the passive wheel using the proposed inverse kinematics overlap the desired trajectory and yaw of the passive wheel. There is a large error between the contact point trajectory using the simple solver without considering the wheel geometry and the desired trajectory along the X-axis on the ground coordinate system. This error can affect the stability of the roller skating speed for the quadrupedal robot.

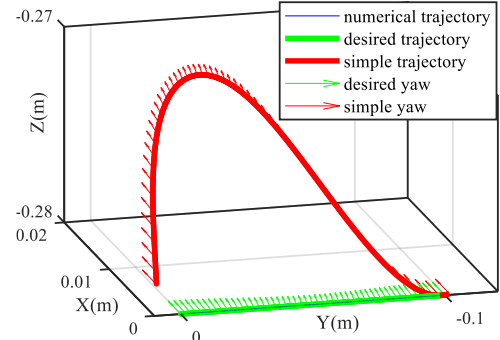


Fig. 9 The position of the contact point and yaw of the wheel on the robot prototype using the trajectory of the Swizzling gait. The numerical trajectory means the contact point trajectory using the proposed inverse kinematics. The simple trajectory and yaw mean the contact point trajectory and yaw using the simple solver without considering the wheel geometry. The numerical and desired trajectory basically overlap.

The numerical iteration number of the proposed inverse kinematics method using the approximate analytical solution as the initial value is less than 6. It takes about 9ms to calculate 100 times the inverse kinematics with the proposed method on the prototype. The proposed inverse kinematics method not only has high precision but also has sufficient computational efficiency to apply to the robot prototype.

B. Roller Skating

The roller skating gaits using the proposed kinematics with the wheel geometry (the Swizzling, Stroking, and trot-like gaits) are verified in the robot prototype. The trajectory of the robot body shown is captured by the 3-D motion-capture system in the ground coordinate system.

The robot body velocity of the linear motion of the roller skating gaits is shown in Fig. 10. The desired velocity of all gaits whose parameters and dynamics controller are the same is 0.4m/s. In the Stroking gait, the robot using the proposed inverse kinematics has a higher acceleration than the robot using the simple inverse kinematics. There is no significant difference in the disturbance along the Y-axis and Z-axis between the two curves. In the Swizzling gait, the robot with the proposed numerical method has a smaller disturbance along the X-axis and Z-axis than the robot with the simple inverse kinematics. The results show the proposed method effectively compensates the motion of the passive wheel and enhances the motion accuracy of the robot. In the trot-like roller skating gait, there is no significant difference between the two curves. This result shows the dynamic gait which uses

the ground thrust to generate the motion is not sensitive to the kinematic accuracy. Based on the experiments of the linear motion between different gaits, the proposed inverse kinematics method can effectively improve the motion accuracy of static roller skating gait but does not significantly improve the dynamic roller skating gait.

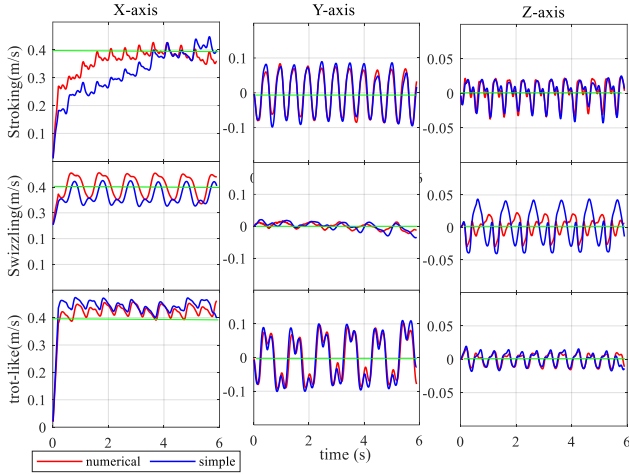


Fig. 10 The robot body velocity of the linear motion of the roller skating gaits. The red and blue curves is the body velocity whose inverse kinematics uses the proposed numerical method and the simple geometry solution. The green curve is the command for robots. The direction of the linear motion is normalized along the X-axis in the ground coordinate system.

The body trajectory of the turning motion of the roller skating gaits is shown in Fig. 11.

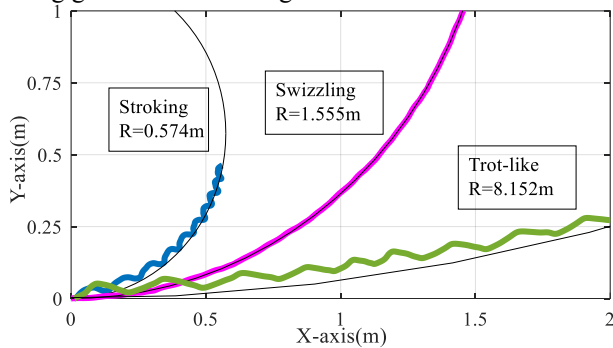


Fig. 11 The body trajectory of the turning motion of the roller skating gaits. The fitting radius of the Strokings, Swizzling and trot-like roller skating gaits are 0.574, 1.555, and 8.152m.

The desired linear velocity of all gaits is 0.4m/s. The experiment result shows the proposed robot can achieve linear and turning motion using the proposed locomotion method and gait design. The Strokings gait can easily achieve the turning motion with a small radius and the trot-like roller skating is difficult to achieve the turning with a small radius. Due to the different ways to generate skating motion of the static and dynamic gaits, the dynamic roller skating gaits make it difficult to achieve the turning motion. The skating motion of the static roller skating gaits is mainly generated by the kinematics of passive wheels and can be controlled by the locomotion design of the robot kinematics. However, the skating motion of the dynamics roller skating gaits is obtained by the linear momentum between the foot and ground which is difficult to transform into angular

momentum. So, the turning motion of the dynamics roller skating gait needs to be a special design that is similar to human roller skating.

C. Energy consumption

The cost of transport (COT) is the important index of the efficiency of the mobile robot and can be expressed

$$COT = \frac{S_0}{G_0 T_0} \quad (10)$$

where S_0 is the mechanical energy consumption of all joints in one cycle and T_0 is the mobile distance of one cycle for the periodic gait. G_0 is the weight of the robot. In this paper, one joint consumption can be computed as $\int |\tau \omega| dt$ where τ and ω are torque and angular velocity of the joint.

The COT of the trot walking, Swizzling, Strokings, and trot-like roller skating gaits are shown in Table 2. The Swizzling, Strokings, and trot-like roller skating decrease the COT by approximately 30% and 50% to the trotting walking gait in the experiments. However, the COT of the trot-like roller skating gait is not significantly lower than that of the static gaits (Swizzling and Strokings). Compared with the previous robot whose each leg has 3-DoFs, the trot walking has no change and the trot-like roller skating increases the COT by about 25%. The fourth joint of each leg has little consumption in walking and high consumption in roller skating to maintain the yaw angle of the passive wheel.

TABLE 2
ROBOT EFFICIENCY

	Trot walking	Swizzling	Strokings	trot-like
COT	0.35±0.01	0.20±0.02	0.28±0.02	0.18±0.02
[1]	0.35±0.02	\	\	0.136±0.028

V. CONCLUSION

A new quadrupedal robot whose each leg has four DoFs and the passive wheel-foot effector is designed to enable various roller skating locomotion (including Swizzling, Strokings, and trot-like gaits). The wheel geometry is considered to improve the precision of roller skating kinematics and the contact point for the dynamics controller. To avoid the singular solution and reduce iterations of the Levenberg-Marquardt method, the approximate solution that ignores the wheel geometry is utilized as the initial value. The position of the robot foot and the yaw angle of the passive wheel are decoupled for motion planning of all proposed gaits. Our proposed kinematics with wheeled geometry and roller skating gaits were verified through experiments to have higher precision, while the feasibility of all proposed roller-skating gaits was confirmed during straight motion and turning motion with a small radius on our prototype robot. The turning radius of different gaits is discussed to find it difficult to achieve the small turning radius for the dynamic roller skating gaits.

We will pay attention to the gait design of the turning motion for the dynamic roller skating and controller to improve the efficiency of the force control.

REFERENCES

- [1] J. Chen, K. Xu, R. Qin, and X. Ding, "Locomotion Control of Quadrupedal Robot With Passive Wheels Based on Col Dynamics on SE (3)," *IEEE Transactions on Industrial Electronics*, 2023.
- [2] N. Eiji and N. Sei, "Leg-wheel robot: a futuristic mobile platform for forestry industry," in *Proceedings of 1993 IEEE/Tsukuba International Workshop on Advanced Robotics*, 1993, pp. 109-112: IEEE.
- [3] R. Buchanan, L. Wellhausen, M. Bjelonic, T. Bandyopadhyay, and M. Hutter, "Perceptive Whole Body Planning for Multi-legged Robots in Confined Spaces," *Journal of Field Robotics*, vol. 38, no. 1, pp. 68-84, 2020.
- [4] Y. De Viragh, M. Bjelonic, C. D. Bellicoso, F. Jenelten, and M. Hutter, "Trajectory Optimization for Wheeled-Legged Quadrupedal Robots using Linearized ZMP Constraints," *IEEE Robotics & Automation Letters*, vol. 4, no. 2, pp. 1633-1640, 2019.
- [5] V. S. Medeiros, E. Jelavic, M. Bjelonic, R. Siegwart, and M. Hutter, "Trajectory Optimization for Wheeled-Legged Quadrupedal Robots Driving in Challenging Terrain," *IEEE Robotics and Automation Letters*, vol. 5, no. 3, pp. 4172-4179, 2020.
- [6] W. Du, M. Fnadi, and F. Benamar, "A new whole-body motion generator and adaptive altitude control for a quadruped-on-wheel robot," *Journal of Mechanisms and Robotics*, vol. 15, no. 4, p. 041005, 2023.
- [7] W. Du, M. Fnadi, and F. Benamar, "Whole-body motion tracking for a quadruped-on-wheel robot via a compact-form controller with improved prioritized optimization," *IEEE Robotics and Automation Letters*, vol. 5, no. 2, pp. 516-523, 2020.
- [8] A. Bouton, C. Grand, and F. Benamar, "Design and control of a compliant wheel-on-leg rover which conforms to uneven terrain," *IEEE/ASME Transactions on Mechatronics*, vol. 25, no. 5, pp. 2354-2363, 2020.
- [9] T. Klamt *et al.*, "Remote mobile manipulation with the centauro robot: Full-body telepresence and autonomous operator assistance," *Journal of Field Robotics*, vol. 37, no. 5, pp. 889-919, 2020.
- [10] M. P. Polverini, E. M. Hoffman, A. Laurenzi, and N. G. Tsagarakis, "Sparse optimization of contact forces for balancing control of multi-legged humanoids," *IEEE Robotics and Automation Letters*, vol. 4, no. 2, pp. 1117-1124, 2019.
- [11] A. Yeldan, A. Arora, and G. S. Soh, "Contact Based Turning Gait of a Novel Legged-Wheeled Quadruped," in *2023 IEEE International Conference on Robotics and Automation (ICRA)*, 2023, pp. 9707-9713: IEEE.
- [12] J. Sun, Y. You, X. Zhao, A. H. Adiwahono, and C. M. Chew, "Towards more possibilities: Motion planning and control for hybrid locomotion of wheeled-legged robots," *IEEE Robotics and Automation Letters*, vol. 5, no. 2, pp. 3723-3730, 2020.
- [13] GenEndo and ShigeoHirose, "Study on Roller-Walker-Improvement of Locomotive Efficiency of Quadruped Robots by Passive Wheels," *Advanced Robotics*, vol. 26, no. 8-9, pp. 969-988, 2012.
- [14] M. Bjelonic, C. D. Bellicoso, M. E. Tiryaki, and M. Hutter, "Skating with a force controlled quadrupedal robot," in *2018 IEEE/RSJ International Conference on Intelligent Robots and Systems (IROS)*, 2018, pp. 7555-7561: IEEE.
- [15] M. Geilinger, R. Poranne, R. Desai, B. Thomaszewski, and S. Coros, "Skaterbots: Optimization-based design and motion synthesis for robotic creatures with legs and wheels," *ACM Transactions on Graphics (TOG)*, vol. 37, no. 4, pp. 1-12, 2018.
- [16] M. Geilinger, S. Winberg, and S. Coros, "A computational framework for designing skilled legged-wheeled robots," *IEEE Robotics and Automation Letters*, vol. 5, no. 2, pp. 3674-3681, 2020.
- [17] J. Chen, K. Xu, and X. Ding, "Roller-skating of mammalian quadrupedal robot with passive wheels inspired by human," *IEEE/ASME Transactions on Mechatronics*, vol. 26, no. 3, pp. 1624-1634, 2020.
- [18] K. Xu, R. Qin, J. Chen, L. Han, and X. Ding, "Design and motion planning of wheel-legged hexapod robot for planetary exploration," *Acta Aeronauticaet Astronautica Sinica*, vol. 42, no. 1, pp. 524244-524244, 2021.
- [19] J. Chen, H. Chen, K. Xu, and X. Ding, "Trot-Like Roller-Skating of Quadrupedal Robot with Passive Wheels," in *2022 IEEE International Conference on Robotics and Biomimetics (ROBIO)*, 2022, pp. 1402-1407: IEEE.
- [20] D. Kim, J. Di Carlo, B. Katz, G. Bledt, and S. Kim, "Highly dynamic quadruped locomotion via whole-body impulse control and model predictive control," *arXiv preprint arXiv:1909.06586*, 2019.
- [21] M. Hosseini, D. Rodriguez, and S. Behnke, "State Estimation for Hybrid Locomotion of Driving-Stepping Quadrupeds," in *2022 Sixth IEEE International Conference on Robotic Computing (IRC)*, 2022, pp. 103-110: IEEE.